ROOT CAUSE ANALYSIS OF AFTERBURN IN RFCC REGENERATOR USING COMPUTATIONAL FLUID DYNAMICS

Mohammad Abdur Rakib[1*], Tommy Firmansyah[1], Syed Basheer[1], Mohamed Al Musharfy[1] and Sam Clark[2]

[1]ADNOC Refining Research Centre, Abu Dhabi National Oil Company (ADNOC) Refining, PO Box 3593, Abu Dhabi, UAE

[2]CPFD LLC, 10899 Montgomery Blvd. NE Suite A, Albuquerque, NM 87111, USA

*Email: *mrakib@adnoc.ae*

Abstract

The regenerator is typically the largest vessel of the Residue Fluid Catalytic Cracking (RFCC) unit, usually operated in the turbulent fluidization regime. In a typical RFCC unit, catalyst regeneration is conducted in a 2-stage regenerator to minimize hydrothermal deactivation of catalyst, due to high Conradson Carbon Residue (CCR) content of the feed. One of problems faced in this regenerator is afterburn or post combustion in the dilute bed region, resulting in high temperatures in the overhead line of the regenerator.

The present study concerns with observed thermal asymmetry and afterburn in a commercial RFCC regenerator, which resulted in reduced RFCC unit severity. Detailed Computational Fluid Dynamics (CFD) model of RFCC regenerator was developed to study the temperature distribution across the dense and dilute phase of the regenerator. This also included the spatial distribution of partly-regenerated catalyst entering the 2nd Stage Regenerator from the 1st Stage Regenerator, and any mal-distribution of air and catalyst in the regenerator.

Uniformity of gas flow is always important for good performance of regenerators, and low uniformity in the dense bed of regenerators is usually associated with afterburn and high levels of NOx emissions. CFD simulation revealed strong bias of higher flow near the axis and the outer wall of the regenerator with very little radial/ lateral velocity components, leading to inefficient mixing of gas and catalyst in the bed, and radial temperature gradient and maldistributions of O2 and CO concentration. The O2-rich air was found streaming near the outer walls and the centre of the dense bed region, and the CO-rich combustion product gases from the dense bed further mixes in the dilute bed region proceeding to complete combustion, leading to further temperature spikes.

Additionally, the distribution of partially regenerated catalyst was revealed to be not optimal. Most of the partially regenerated catalyst goes directly upward from the catalyst distributor without significant lateral distribution, further aggravating the problem.

Introduction

Good temperature distribution across the dense bed of the RFCC regenerator is important to maintain catalyst regeneration and recovering the catalyst activity. One of major problems faced in the regenerator is afterburning or post combustion problem with the presence of abnormally high temperatures in the overhead line of the regenerator. This paper presents root cause analysis (RCA) study of afterburn in an industrial RFCC regenerator.

A computational model was constructed, executed, and analyzed using a commercial Computational Fluid Dynamics (CFD) software specialized in highly densed particulate system called Barracuda Virtual Reactor (VR).

The primary focus of the analysis was mixing of air and partially-regenerated catalyst in the 2nd stage regenerator dense phase and afterburn in the dilute phase.

Modeling Approaches

Barracuda VR is based on Lagrangian-Eulerian approach called Multiphase Particle-in-Cell (MP-PiC), which was first introduced by Snider (2001, 2007) and O'Rourke et. al (2009). The gas phase is represented as continuum Eulerian whereas the solid particles phase is represented by Lagrangian discrete particles with strong coupling between both phases. It solves the transient fluid and particle mass, momentum and energy equations in three dimensions. Particles-particles interaction is modeled with collision stress, based on lumping particles in numerical parcels.

A 3D solid model of the RFCC 2nd stage regenerator was created, as shown in the left of Figure 1. All major components were explicitly modelled including cyclones and diplegs, outlets to withdrawal wells, catalyst cooler withdrawal, air rings, spent catalyst distributor, and catalyst cooler return. The computational mesh comprises 870K cartesian cells, as shown in the right of Figure 1.

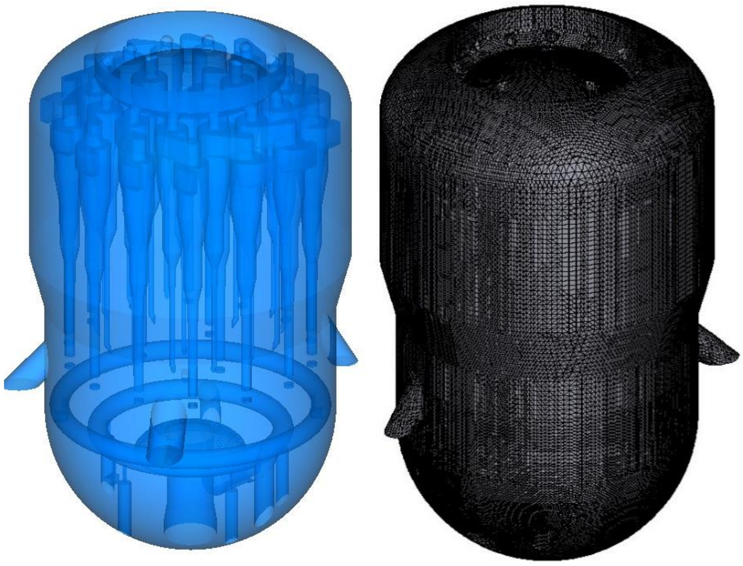

Figure 1. Geometry and Computational Mesh of RFCC 2nd Stage Regenerator.

Air is introduced through the lift line, catalyst cooler distributor, air ring distributors, and vents above the withdrawal wells and catalyst cooler withdrawal. Particles were initialized in the system following the catalyst bed inventory at the actual operation.

The model assumes that all hydrogen has been burned off the particles in the 1st stage regenerator and that only carbon remains in the coke that enters the 2nd stage regenerator. Therefore, the initial particle bed only had carbon components in the coke, with 0.02% coke on catalyst. The catalyst and gas flow from the 1st stage regenerator lift line was introduced through 8 flow boundary conditions at the mushroom distributor window locations.

The fluid flow into the system is assumed to be 100% air with a relative humidity of 50%. Particles exited the regenerator through a particle exit flow boundary condition on the catalyst cooler withdrawal well and returned via the cooled catalyst distributor flow boundary condition.

There are two air distributor rings; an inner and an outer air ring. The inner air ring is at a lower elevation than the outher air ring. This was represented by injection boundary condition at the location of each nozzle.

The regenerator has an outer ring of 17 sets of cyclones and an inner ring of 3 sets of cyclones. Each set comprises a first and second stage cyclone. The model assumes 100% efficiency of the cyclones, so all particles exiting the pressure boundary conditions were returned to the first and second stage dipleg flow boundary conditions.

Chemical reactions were modelled with a simplified set of chemical equations. The chemistry was taken from Arbel et. al. (1995) whilst the coke combustion kinetics set was based primarily on the work of Weisz (1966) and Weisz and Goodwin (1966).

Results and Discussions

Figure 2 shows time averaged of different resulting variables along the middle vertical cross-sectional plane. It provides a good overview of flow pattern and overall behavior of particles solid concentration, gas temperature, along with O_2, CO_2 and CO concentration.

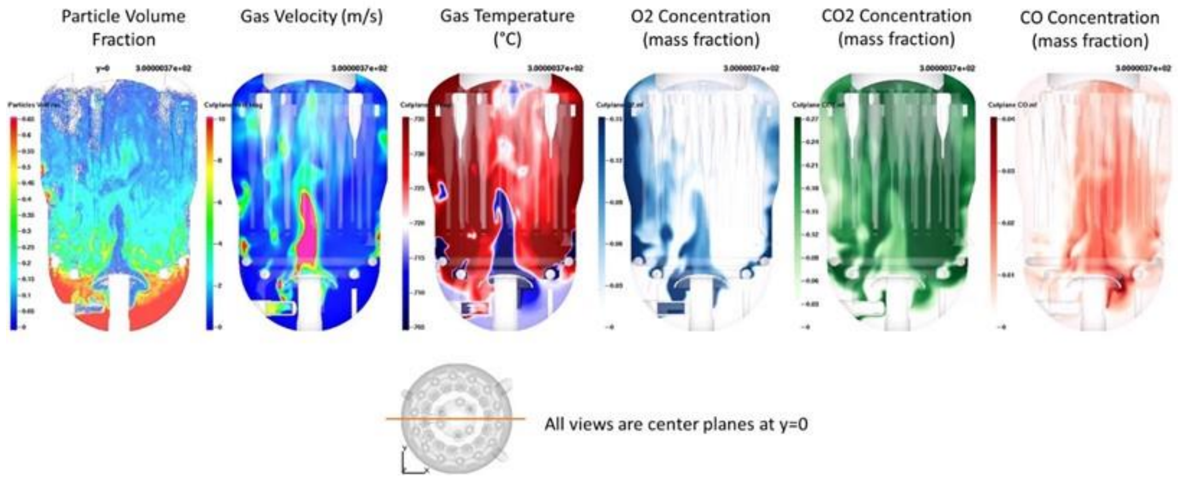

Figure 2. Resulting Variables.

A clear distinct feature of the flow pattern appears at the core and near the outer wall of the 2nd Stage Regenerator. This is highlighted in the high gas velocity regime downstream of the central mushroom distributor and the outer air ring, as shown in the second picture from the left in Figure 2.

As a result of this strong flow regime, most of the solids particles drawn to this region are immediately swept upwardly. Figure 3 shows the impact of the high gas velocity to the solids particle concentration.

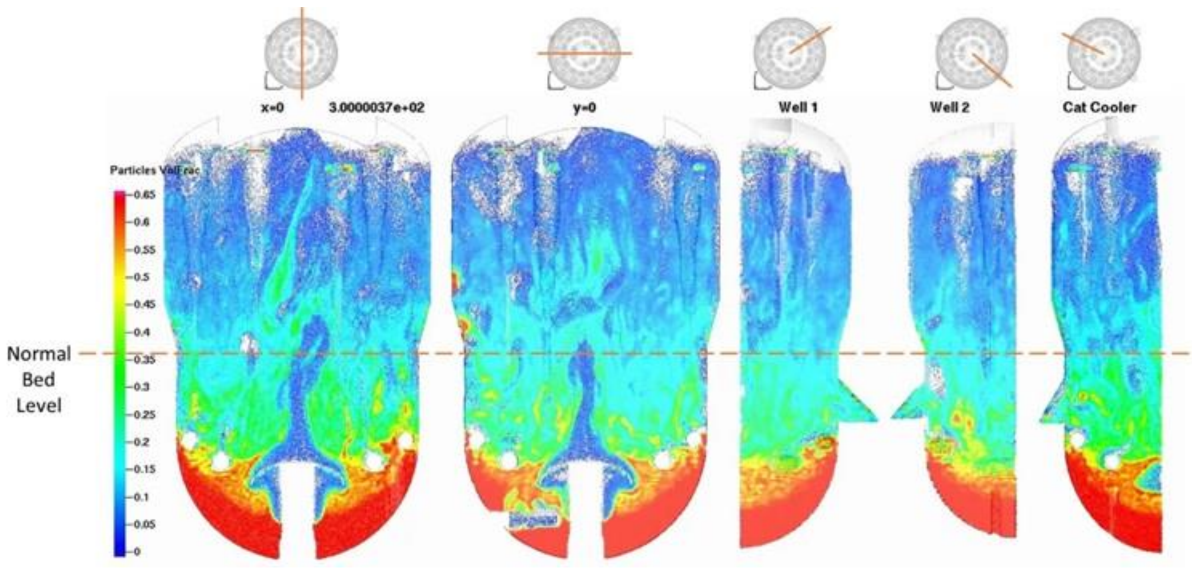

Figure 3. Resulting Solids Particle Concentration.

Movement of catalyst particles are mostly influenced by gas flow stemming from the partially burnt catalyst distributor, i.e. mushroom distributor with underneath lateral window slots, catalyst cooler return distributor and air ring distributors. As the gas flow tends to push axially with no significant radial or lateral component, it thus leads to major stagnant region of catalyst particles at the base of the 2nd Stage Regenerator, as depicted clearly in Figure 3. The stagnation of catalyst could also be due to the inability of Barracuda to model particle-wall stresses correctly resulting in catalyst packing at the wall. The high density zones at the bottom could be caused by the above two factors. Which factor dominates was not the subject of this investigation. Furthermore, the solid volume fraction profile is not uniform above the mushrooom and air ring distributors, showing inefficient mixing of gas and catalyst in the bed.

The non-uniformity of gas flow pattern has also led to mal-distribution of O_2 and CO and temperature gradient across the 2nd Stage Regenerator, as shown in Figure 4. O_2 breakthrough in the dense bed region is clearly visible at the core and near the outer wall following strong axial gas flow from the mushroom distributor and the outer ring distributor, respectively. On the other hand, the CO concentration tends to present more significantly at the core region going into the inner cyclones. This CO imbalance may potentially lead to afterburn problem in the dilute phase as well as the flue gas line when localized combustion of CO with O2 occurs and causes temperature spikes.

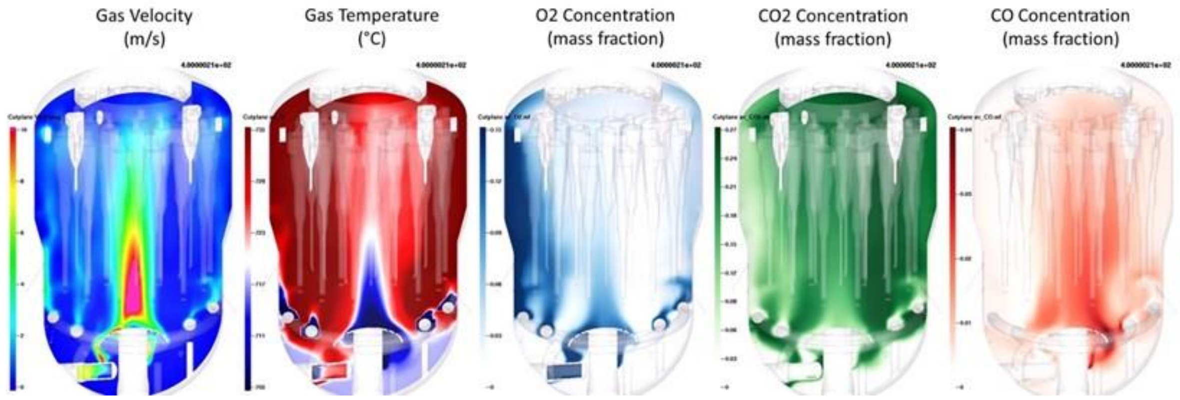

Figure 4. Time Averaged Axial Distribution.

Gas temperature distribution in Figure 4 shows similar pattern to that of velocity, with relatively cool temperature near the air grid distributors (mushroom and air rings). The gas quickly heats to the regenerator operating temperature in the dilute phase where the catalyst density is low.

Figure 5 shows the distribution of partiallly regenerated catalyst from the 1st Stage Regenerator after entering through the mushroom distributor. The color represents the particles residence time with the upper scale (red) showing the residence time of 10 seconds and above. The high gas axial velocity obviously pushes the partly regenerated particles immediately upward as soon as it enters the lateral window slots in the lift line and passes through the mushroom distributor. This again illustrates that the distribution of spent catalyst in the dense bed is poor due to very little lateral mixing of catalyst into the dense bed.

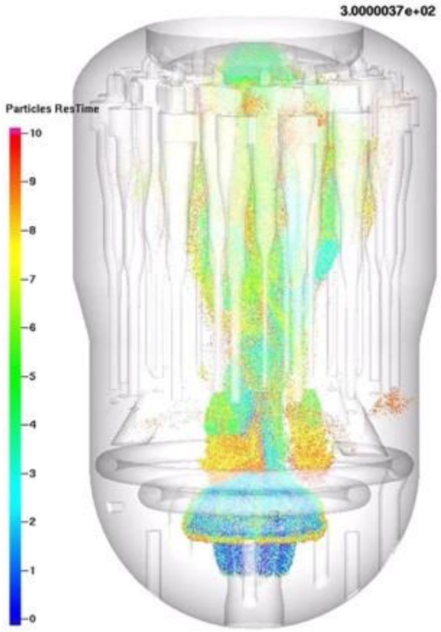

Figure 5. Particles Residence Time of Partially Regenerated Catalyst.

Conclusions

The simulation results revealed strong bias of flow at the core and the outer wall of the 2nd Stage Regenerator with very little radial/ lateral velocity components. This in turn led to inefficient mixing of gas and catalyst in the bed, temperature gradient and maldistribution of O2 and CO concentration. Afterburn and thus temperature spike along the dilute phase and flue gas line is likely due to O2-rich air which streams near the outer walls contacting CO-rich combustion gases near the center.

References

Arbel, A., Huang, Z., Rinard, I. H., Shinnar, R. Dynamics and control of fluidized catalytic crackers. 1. Modelling of the current generator of FCC's. Industrial & Engineering Chemistry Research, 1995. 34, 1228-1243.

O'Rourke, P. J., Zhao, P., Snider, D. M. A model for collisional exchange in gas/liquid/solids fluidized beds, Chemical Engineering Science, 2009. 64, 1784-1799.

Snider, D. M. An incompressible three-dimensional multiphase particle-in-cell model for dense particle flows, Journal of Computational Physics. 2001. 170, 523-549.

Snider, D. M. Three fundamental granular flow experiments and CPFD predictions, Powder Technology. 2007. 176, 36-46.

Weisz, P. Combustion of carbonaceous deposits within porous catalyst particles. III. The CO_2/CO product ratio. Journal of Catalysis. 1966. 6, 425-430.

Weisz, P., Goodwin, R. Combustion of carbonaceeous deposits within porous catalyst particles. II. Intrinsic burning rate. Journal of Catalysis. 1966. 6, 227-236.